

Microheterogeneity of Local Segment Mobility in Solid Polymethacrylates As Studied by a Polymer-Bound Twisted Intramolecular Charge Transfer Chromophore

Rong Kun Guo¹ and Shigeo Tazuke*

Research Laboratory of Resources Utilization, Tokyo Institute of Technology,
4259 Nagatsuta, Midori-ku, Yokohama 227, Japan. Received May 10, 1988;
Revised Manuscript Received December 6, 1988

ABSTRACT: A trace amount of (dimethylamino)benzoate (DMAB) chromophore as a TICT (twisted intramolecular charge transfer) fluorescence probe is bonded to poly(methyl methacrylate) with different spacer lengths and to poly(alkyl methacrylate)s (alkyl = methyl, butyl, and cyclohexyl) with a dodecyl group. The fluorescence and absorption spectra of the polymers were studied in solid films. The relative concentration of the TICT state is expressed by the ratio (R) of the emission intensity from the TICT excited state (a^*) to that from the local excited state (b^*). The R value decreases with the decrease in the spacer length between the DMAB group and the main chain as well as with the increase in the bulkiness of adjacent polymer side chains. The red edge excitation (REE) effect was also observed, inferring the ground-state conformational distribution. The absorption and excitation spectra provide further evidence on the dependence of the ground-state conformation on the chromophore location in the polymer and also on the polymer structure. Fluorescence polarization of the a^* and b^* bands provides information on steric constraint reflecting on orbital mixing which also supports the conclusion derived from other measurements. The present results explicitly indicate the presence of microheterogeneity in the solid polymer.

Introduction

The effect of the microenvironment on molecular mobility, orientation, and conformation in solid polymers is a novel topic relevant to the basic understanding of chemical reactivity in the solid state. This line of study is expected to provide a guiding principle for the design of various specialty polymers in which diffusion of functional groups in the solid state is required. It is a matter of course that the total segment motion is liberated above the glass transition temperature (T_g) of the polymer. If local segment motion can be released much below T_g by means of introducing a long spacer group connecting a particular functional group to the main chain, it would be beneficial for the design of specialty polymers in which bimolecular or diffusional process are required. These include photoresists, polymer-supported catalysts, membranes for active transport, and so forth.

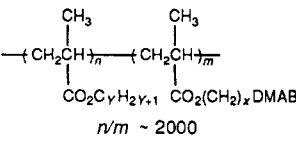
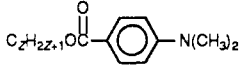
In the preceding studies, we have demonstrated that the side-chain mobility in polymethacrylates is subject to the steric effects owing to the main chain as well as to the neighboring side chains in dilute solutions.^{2,3} For example, when an extremely small amount of long alkyl chain is incorporated in poly(methyl methacrylate), the segment mobility at the end of the long alkyl chain depends very much on its length. For the study of such minor local sites, the fluorescence method is most suitable. Fluorescence methods, such as steady-state fluorescence spectroscopy, fluorescence depolarization, excited-state decay analysis, and time-resolved fluorescence spectroscopy, have been accepted as effective tools in the investigation of the microenvironment around a chromophore.^{4,5}

A number of molecular mobility probes useful in solution systems have been developed. However, when one intends to apply these methods in the solid state, the main difficulty is the limited freedom of molecular motion. Apparently, exciplex or excimer formation cannot be used. Exciplex formation occurring at a distance of 7–8 Å is expected to be less susceptible to diffusion processes than excimer formation, requiring a face-to-face alignment at a separation of 3–4 Å.⁶ Even so, exciplexes are not effectively formed in polymer matrices since the donor-acceptor diffusion process cannot be fulfilled within the fluorescence lifetime.⁷

Twisted intramolecular charge transfer fluorescence (TICT)⁸ would be more suitable for solid-state study. TICT phenomena are sensitive to the local viscosity and local polarity. Furthermore, the mode of molecular motion leading to TICT formation is suitable to study the available free volume in polymer matrices, because the rotation is well limited around a particular bond and the size of rotor can be selected.⁹ This type of fluorescence probe has been proved to be useful in dilute to very viscous polymer solutions.^{10–12} The advantages of the probe are as follows. First, a clear dual fluorescence can be observed. Second, the rotational motion leading to the dual fluorescence seems to require a rather small free volume and is well limited around a special nitrogen–benzene bond so that both polymer-bound and free probe exhibit the same TICT properties in the same environment. Third, since the fluorescence sensor is very sensitive, a trace amount of DMAB (<0.04%) is enough to check the environmental effect and does not alter the bulk polymer properties. Fourth, in addition to emission spectroscopy, the phenomenon called the red-edge excitation (REE) effect also provides qualitative information on the ground-state conformational distribution controlled by the surrounding media.^{13,14} With the use of the TICT fluorescence probe, we are trying to present unequivocal evidence in support of the presence of site-specific free volume. It would then be possible to design a rigid polymer with a sufficient free volume pool at the desired site for a chemical reaction to occur.

The concept of microscopic heterogeneity of free volume distribution in polymer matrices has been put forward by phosphorescence decay analysis.^{15,16} However, since a phosphorescence probe is mixed in polymer matrices, it is very difficult to identify the location of the probe. To have an inside look into the problem of site-selective free volume along a linear polymer chain, the probe for molecular mobility should be chemically bonded to a well-defined site in the polymer. Azobenzene analogues as free volume sensitive photochromic labels have been used as initiator/cross-linker of epoxy resin to evaluate free volume at various sites in glassy polymers¹⁷ and also to probe free volume at the chain end, the middle of main chain, and the side chain of polystyrene.¹⁸ Apart from the photo-

Table I
Structures and T_g s of Polymers and Monomer Compounds

structure	X	Y	Z	abbreviation	$10^4 M_n^a$	$T_g, ^\circ\text{C}$
	2	1		poly(MMA-co-2)	10	122
	4	1		poly(MMA-co-4)	10	122
	8	1		poly(MMA-co-8)	5.5	122
	12	1		poly(MMA-co-12)	10	121
	12	4		poly(BMA-co-12)	5.5	22
	12	6 ^b		poly(CHMA-co-12)	5.0	97
	12	12		poly(DDMA-co-12)	5.0	
			2	EDMAB		
			4	BDMAB		
			8	ODMAB		
			12	DDDMAB		

^a M_n was determined by GPC measurement with monodispersed polystyrenes as the standard. ^b For cyclohexyl group, the number of hydrogens is 2Y.

chromic technique, the fluorescence method is an extremely sensitive method to probe minute differences in polymer environment. Since the pioneering work by Morawetz, the homogeneous mixing and phase separation problem has been widely studied by energy-transfer techniques.^{4,5,19} Interpenetration of polystyrene chains in solution and film was recently studied by this method, using the combination of polymer-bonded carbazole and anthracene.²⁰

In the following, we are presenting the spectroscopic results on a series of polymethacrylates in the solid state. A trace amount of (dimethylamino)benzoate (DMAB) chromophore as a TICT fluorescence probe was tagged to poly(methyl methacrylate) with various spacers and to poly(alkyl methacrylate) with dodecyl group as a spacer, whereas the alkyl side chain is different (Table I). Our interest lies on the information on how the small structural differences affect fluorescence behaviors through which microheterogeneity in amorphous polymers can be examined. Comparison between dilute solutions^{2,3} and the solid state is another point of interest in view of investigating the role of solvents on polymer segment motion.

Experimental Section

Materials. Poly[(methyl methacrylate)-co-[2-[[4-(dimethylamino)benzoyl]oxy]ethyl methacrylate]] [poly(MMA-co-2)], poly[(methyl methacrylate)-co-[4-[[4-(dimethylamino)benzoyl]oxy]butyl methacrylate]] [poly(MMA-co-4)], poly[(methyl methacrylate)-co-[8-[[4-(dimethylamino)benzoyl]oxy]octyl methacrylate]] [poly(MMA-co-8)], poly[(methyl methacrylate)-co-[12-[[4-(dimethylamino)benzoyl]oxy]dodecyl methacrylate]] [poly(MMA-co-12)], poly[(butyl methacrylate)-co-[12-[[4-(dimethylamino)benzoyl]oxy]dodecyl methacrylate]] [poly(BMA-co-12)], and poly[(cyclohexyl methacrylate)-co-[12-[[4-(dimethylamino)benzoyl]oxy]dodecyl methacrylate]] [poly(CHMA-co-12)] were prepared in our laboratory. The synthesis and sample characterization were reported previously.^{2,3,11} The glass transition temperature (T_g) was measured by a differential scanning calorimeter (DSC) (Seiko DSC 100) and the data were collected in Table I. The results show that the T_g of a polymer containing a small amount of the probe is always same as the value for the relevant unlabeled polymer.

The polymer films were prepared by solution casting. A 3% polymer solution in ethyl acetate was coated on a clean quartz plate (24 × 19 mm), then dried at room temperature for 12 h, and further evacuated in a vacuum desiccator. All polymer films were annealed at about 10 °C above the T_g under nitrogen atmosphere for 2 h and cooled gradually for 3–4 h.

The polymer films doped with monomer model compound, dodecyl 4-(dimethylamino)benzoate (DDDMAB), were similarly prepared and used as reference samples. The content of dopant is about 0.04 wt %. The host polymer, poly(methyl methacrylate) (PMMA), was prepared by radical polymerization and the number-average molecular weight (M_n) was determined to be 4×10^5 , by GPC (HLC-802, Toyo Soda). The influence of casting con-

ditions on the fluorescence behaviors of polymer films was carefully examined. The effects of coating solvents, coating temperature, and polymer concentration did not affect the results.

Spectroscopy. Absorption spectra were recorded on a Hitachi 320 spectrophotometer. Fluorescence emission and excitation spectra and fluorescence polarization were recorded on a Hitachi F-4000 spectrofluorometer. Fluorescence polarization measurements in the solid polymer film often lead to erroneous results. The data were not corrected for polarization characteristics of the monochromator so that the absolute value of polarization (P) might contain some errors. For the present purpose, comparison among samples on a relativistic scale is needed and the data are quite reliable in this aspect. All emission spectra were corrected by a built-in computer for wavelength-dependent sensitivity of the spectrometer. For the measurement of excitation spectra, the slit width for excitation and emission light is kept at 3 nm. The background emission intensity due to impurities in the films was less than $1/20$ of that of the DMAB chromophore for the excitation around 300 nm.

Results and Discussion

Influence of Polymer Main Chain and Adjacent Side Chains on the Emission Intensity Ratio R . The fluorescence spectra of these copolymer films (Figure 1) show that the intensity of the long-wavelength TICT emission (a^* state) is much weaker than those in solution. Here we used ethyl acetate as solvent, whose molecular structure is similar to that of polyMMA and which is good solvent for the polymer.^{2,3} It is apparent that the mobility of side chains is considerably lost in the solid state. Although the a^* band is not observed as an independent peak, the magnitude of R is adopted as a relative measure of molecular mobility at a particular site ($I_{420\text{nm}}/I_{\lambda_{\text{max}}}$). The R value as a function of the carbon number (X) in the spacer connecting a DMAB group to the polymer main chain and of the carbon number (Y) in the neighboring side chains is shown in Figure 2.

A general tendency is that the R value decreases with reducing the spacer length or increasing the size of the adjacent side chains. The decreasing sequences coincide fully with those established in the dilute solutions.^{2,3} It is easily understandable that when the TICT chromophore approaches the main chain or is surrounded by bulky adjacent side chains, the local free volume in the vicinity decreases and the restriction on the rotational motion leading to TICT state in solid state increases. The temperature dependence of the R value is measured for these polymers revealing that R continuously increases with temperature up to 120 °C. The formation of the TICT state is consequently irreversible and kinetically controlled in the polymer matrix in the temperature range examined.^{9,10} The polymer microenvironmental effect is to govern the rate of TICT state formation. Two characteristics should be mentioned in Figure 2. First, the in-

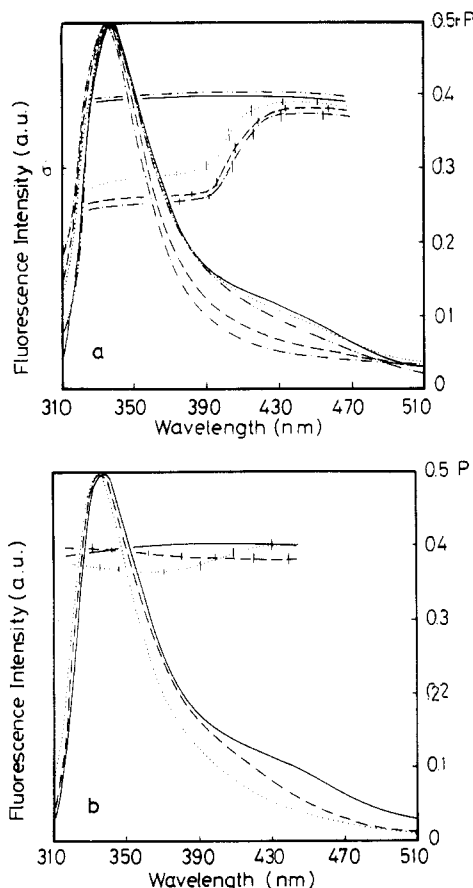


Figure 1. Fluorescence spectra and fluorescence polarization (P): (a) poly(MMA-co-2) (---), poly(MMA-co-4) (---), poly(MMA-co-8) (---), poly(MMA-co-12) (—), and PMMA film doped with DDDMAB (---); (b) poly(MMA-co-12) (—), poly(BMA-co-12) (---), and poly(CHMA-co-12) (---) in the solid state; excitation at 300 nm for fluorescence spectra and at 280 nm for polarization.

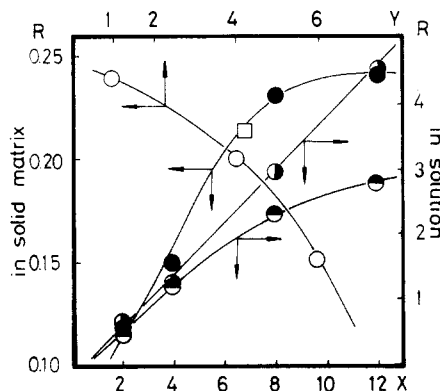


Figure 2. Comparison of R values in solid and solution as a function of the carbon number (X) in the spacer length connecting DMAB to the PMMA main chain (●) and the carbon number (Y) in the neighboring side chain (○): (□) DDDMAB doped in PMMA film; (●) in EA; (●) in BuCl, concentration 1 wt %. The data in solution are taken from ref 2 and 3.

tensity ratio R increases sharply with increasing spacer length in a certain range and then becomes almost constant, so that a plateau in the plot of R as a function of carbon number X is observed. We have reported that the R value seems to level off in poor solvents but not in good solvents. This phenomenon has been explained as due to the fact that the side chain is entrapped into the shrunken polymer chain in poor solvent.² This tendency is enhanced in the solid state, probably attributable to more a restricted chain conformation and a much more compact polymer

stack. Second, although the T_g of all samples are greatly different, the R values seem to be mainly determined by the size of neighboring side chains but not by the mobility of the main chain. T_g does not play a dominant role as in the case of the bimolecular interaction systems such as exciplexes and excimers.^{21,22a} The R value changes gradually around T_g but not sharply. Similarly, a gradual change of maximum emission wavelength in the region of T_g was reported for another TICT compound, 1-phenyl-4-[(4-cyano-1-naphthyl)methylene]piperidine, in a polymer matrix.²³ These observations are in support of the fact that the formation of a TICT state requires a partial rotation of the functional group around a single bond and is not directly relevant to the translational motion of the polymer mass center and the segmental rotation in the backbone of polymer chain permissible only above T_g .^{22b} When a large segment motion is involved, the picture is totally different. For example, Farid et al. found that exciplex fluorescence by 1-pyrenyl-3-[4-(dimethylamino)phenyl]propane requiring interaction between chromophores is much weaker in the polymer matrix at low temperature but almost same at temperatures above T_g compared with those in fluid media.²⁴

Red Edge Excitation (REE) Effect of TICT Phenomena. Examples of the excitation wavelength dependence of fluorescence spectra are shown in Figure 3 for poly(MMA-co-2), poly(MMA-co-12), and poly(CHMA-co-12). When the excitation wavelength is moved to the red, two main changes are observed. (1) The relative magnitude of TICT fluorescence intensity expressed by R increases. (2) The maximum emission wavelength, λ_{\max} , of the b^* band continuously shifts to the red. It is explicitly shown that the magnitudes of both changes are dependent of the spacer length to the main chain and the structure of the neighboring side chains.

In the previous papers^{2,3}, we used a parameter η_R to evaluate the relative magnitude of REE, where η_R is defined as a ratio of the difference between the R value excited at λ (nm) and that at 280 nm to the latter:

$$\eta_R = \frac{R_\lambda - R_{280\text{nm}}}{R_{280\text{nm}}}$$

Figure 4 shows the relations between η_R and the excitation wavelength for the two sets of copolymers. The sequence of REE is as follows: poly(MMA-co-2) > poly(MMA-co-4) > poly(MMA-co-8) > poly(MMA-co-12) and poly(CHMA-co-12) > poly(BMA-co-12) > poly(MMA-co-12). This decreasing sequence agrees well with that established in dilute solution.^{2,3} As shown in Figure 3, the magnitude of the red shift of λ_{\max} of the b^* band for poly(MMA-co-12) is smaller than those for poly(MMA-co-2) and poly(CHMA-co-12). Obviously, the magnitude of REE is dependent on the spacer length between the DMAB group and the main chain and the bulkiness of the neighboring side chains.

The REE effect of the TICT fluorescence comes in effect in rigid or highly viscous media when the exchange rate between individual conformers is slow enough to be comparable to the fluorescence lifetime. When the dimethylamino group is twisted from the molecular plane of the phenyl ring in the ground state, the excited state has easier access to the TICT state. In fact, Rettig et al. have established the relation between the rate of TICT state formation and the ground-state twisted angle of the dimethylamino (DMA) group to the benzene ring for (dimethylamino)benzonitrile (DMABN).^{9,25} The sequence of presently observed REE revealed that the ground-state conformational distribution of the DMAB chromophore

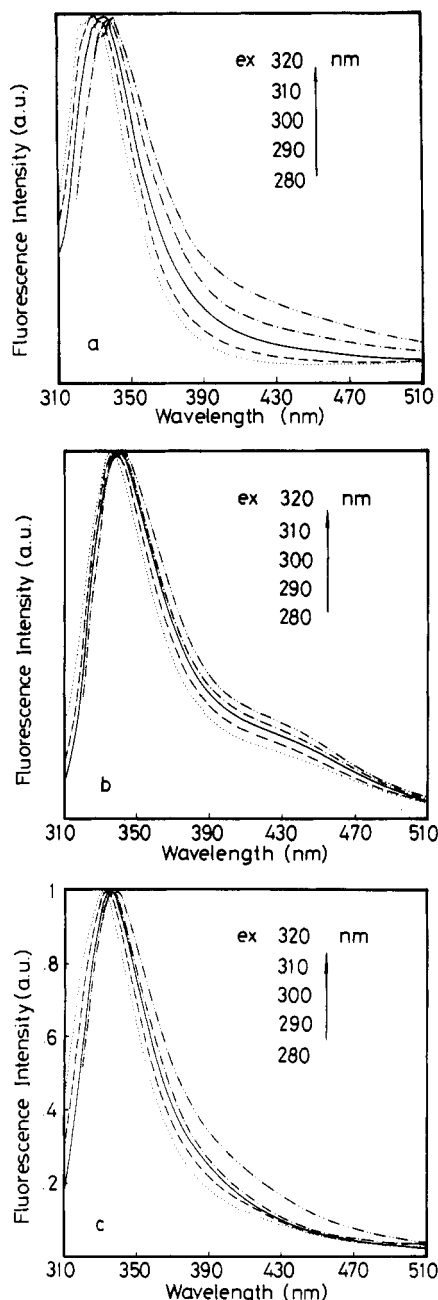


Figure 3. Examples of excitation wavelength dependence of fluorescence. Sample: poly(MMA-co-2) film (a), poly(MMA-co-12) (b), and poly(CHMA-co-12) (c).

attached to polymethacrylate side chain is also subjected to the steric effect of the main chain as well as those of the neighboring side chains in the solid state. When the DMAB group is close to the main chain or surrounded by bulky neighboring side chains, steric constraint seems to favor a broader distribution of the twisting angle in the ground state. This discussion is supported by the results of absorption and excitation spectra described in the following section.

The presence of a REE effect in polymeric systems in general complicates the use of this TICT fluorescence probe. It is not meaningful to compare the results unless the sample is excited at the same wavelength.

Excitation and Absorption Spectra of a DMAB Group Bonded to Polymers. Examples of excitation spectra are shown in Figure 5 for two sets of polymers. When the monitoring wavelength is changed from 400 to 350 nm, the excitation spectra broaden and the peaking wavelengths shift to higher energy. The magnitude of the

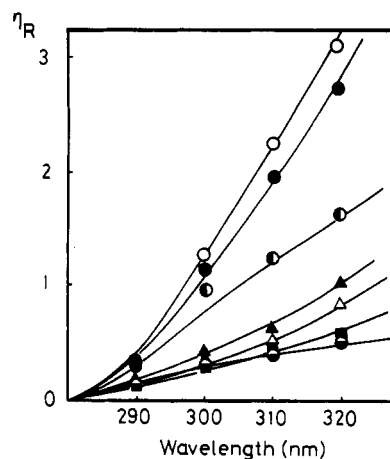


Figure 4. Relation between η_R and the excitation wavelength for poly(MMA-co-2) (○), poly(MMA-co-4) (●), poly(MMA-co-8) (○), poly(MMA-co-12) (●), poly(BMA-co-12) (Δ), poly(CHMA-co-12) (▲), and DDDMAB doped in PMMA (■).

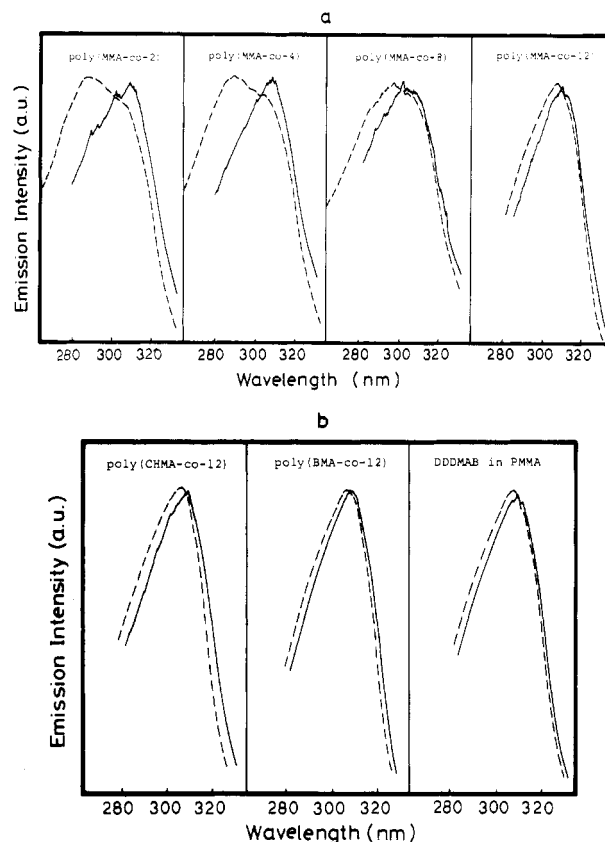


Figure 5. Fluorescence excitation spectra of polymer samples in the solid state: (—) monitored at 400 nm; (---) monitored at 350 nm. (a) (left to right) Poly(MMA-co-2), poly(MMA-co-4), poly(MMA-co-8), poly(MMA-co-12); (b) (left to right) poly(CHMA-co-12), poly(BMA-co-12), DDDMAB in PMMA.

broadening and blue shift is controlled by the polymer main chain and the adjacent side chains. For poly(MMA-co-2) and poly(MMA-co-4), a new band appears at about 275 nm. Corresponding changes have been found in the absorption spectra (Figure 6) for poly(MMA-co-2), in which DMAB groups are fixed close to the main chain, only a shoulder peak appears at about 300 nm. A similar but much lesser broadening of excitation and absorption spectra has been observed in dilute solution.^{2,3} Since the background absorption by the ester groups in polymethacrylates is comparable for all polymers, the difference in absorption spectra should be ascribed either to the shift of absorption band or to the appearance of a new band.

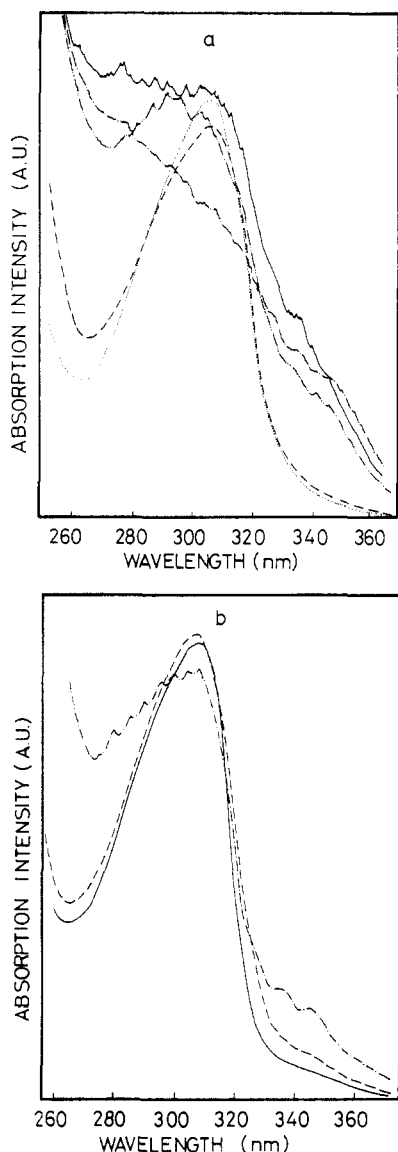


Figure 6. Absorption spectra of polymer films: (a) poly(MMA-co-2) (---), poly(MMA-co-4) (—), poly(MMA-co-8) (····), poly(MMA-co-12) (-·-·-), and 1×10^{-5} M DDDMAB doped in PMMA (-·-·-); (b) poly(MMA-co-12) (—), poly(BMA-co-12) (---), and poly(CHMA-co-12) (····).

Comparison of the absorption spectra (Figure 6) with the excitation spectra (Figure 5) suggests that the spectral changes in poly(MMA-co-2) and poly(MMA-co-4) are to be attributable to the appearance of a new band brought about by the steric constrain on the chromophore. This is a characteristic phenomenon in solid state.

Similar phenomena of spectral shift and dual excitation spectra in polymer matrices have been reported for (dimethylamino)benzonitrile (DMABN) in poly(vinyl alcohol)²⁶ or other protic polymers²⁷ and *p*-piperdylbenzonitrile in PMMA.¹⁴ The appearance of two absorbing species, one mainly responsible for the a^* band and another mainly for the b^* band, indicates that the mode of electronic transition is dependent on polymer structure. There have been published a number of discussions on the topics of the mixing of 1L_a with 1L_b , the participation of $^1(n,\pi^*)$ besides $^1(\pi,\pi^*)$, which are not always unambiguous.^{28,29} Our present aim is not to discuss the assignment of spectra and we will skip all discussions.

Fluorescence Polarization. The preceding discussion on the polymer structural effect on absorption and excitation spectra is reinforced by the fluorescence polarization study. In an ideal case, when the a^* and the b^* bands are

perpendicularly polarized (i.e., the transition moment of a^* is parallel to the long molecular axis whereas that of the b^* band is perpendicular to the long molecular axis) the degree of polarization at the b^* band should be greatly different from that at the a^* band in a solid matrix. However, this is usually not the case for TICT compounds in general. Fluorescence polarization measurement in ethanol at 140 K²⁵ has revealed that DMABE has a flat polarization of ca. 0.4, indifferent of the monitoring wavelength, whereas *p*-(dimethylamino)benzonitrile (DMABN) shows a higher P value at the a^* band than the value at the b^* band. The result of *p*-(dimethylamino)benzoate (DMAB) is surprising. Also the result of DMABN is unexpected since the P value at the b^* band stays at the level of 0.2 which is apparently too high. It has been suggested that the b^* band of TICT compounds containing strongly electron-accepting groups is assigned to the emission from 1L_a . With decreasing the acceptor character of para substituent, the charge transfer character decreases and hence the character of the b^* band approaches that of 1L_b , bringing about reduction in the P value.

Keeping the relation between the CT character and the P value of the b^* emission in mind, we can develop an informative discussion as follows. The data shown in Figure 1 indicate that the wavelength dependence of the P value depends very much on the polymer structure as well as on the spacer length connecting the TICT probe to the polymer main chain. For the polymers having large R values, the P value is constant, indifferent of the monitoring wavelength (poly(MMA-co-12), poly(BMA-co-12), and DDDMAB in PMMA). This behavior is similar to what is observed in a DMAB/ethanol soft glass, indicating the donor-acceptor nature of the compound to be operative on the b^* emission. With increasing steric hindrance to the TICT probe, the P value at the b^* band decreases and the P versus wavelength plots resemble those of DMABN in viscous ethanol. This is a manifestation that the nature of the b^* band is determined by steric effect. Namely, the TICT probe under steric constrain will be distorted so that charge transfer nature in the b^* band is reduced. The sequence of P values at 350 nm shown in Figure 1a agrees very well with the expected steric effect. The effect of polymer structure is not clearly discernible in Figure 1b. However, the most congested polymer, poly(CHMA-co-12), shows a weak tendency of a reduced P value at the lower wavelength region: P values at 350 nm, poly(MMA-co-12) > poly(MMA-co-8) > poly(MMA-co-4) > poly(MMA-co-2).

The observed trend of P values is in good agreement with the results in Figure 5. When both a^* and b^* bands have the same polarization of fluorescence as in the case of poly(MMA-co-12) and DMABE in PMMA, the excitation spectra are nearly independent of the monitoring wavelength, indicative of the presence of single ground-state conformer. For congested polymers represented by poly(MMA-co-2), the presence of two distinctively different absorbing species for the formation of a^* and b^* states correspond to the different degree of fluorescence polarization for the a^* and b^* bands.

Figure 6 demonstrates also the role of steric hindrance, shifting the absorption to a shorter wavelength region.

Monomer Model Compound DDDMAB Doped in PMMA. A very small amount of dodecyl (dimethylamino)benzoate (DDDMAB) doped in PMMA is used as a reference sample to interpret the role of a chemically bonded fluorescence probe in the solid state. The location of a free guest molecule in the polymer matrix will be

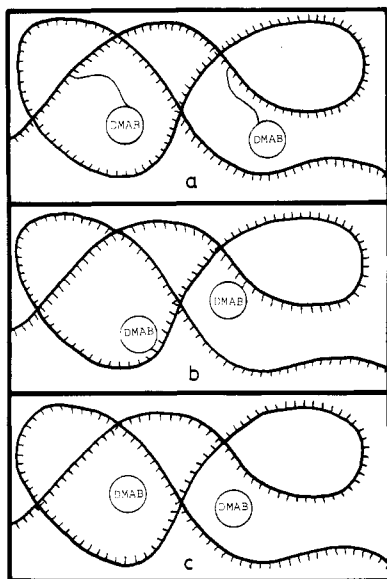


Figure 7. Simplified schematic sketch illustrating the microheterogeneity in amorphous polymer solid: (a) poly(MMA-co-12); (b) poly(MMA-co-2); (c) PMMA + DDDMAB.

different from those bonded to polymers. As shown in Figure 1, the fluorescence of DDDMAB in PMMA resembles those of poly(MMA-co-12) and poly(MMA-co-8). A close look of the R value in Figure 2 and the magnitude of the REE effect in Figure 4 indicates that the guest model molecules are slightly less mobile than poly(MMA-co-12). When the monitoring wavelength is changed from 400 to 350 nm, the blue shift in the excitation spectra (Figure 5) is comparable to that of poly(MMA-co-12). The present results imply that the free guest molecule does not seem to locate at the site of the maximum free volume or the spacer connecting the probe to the main chain brings about an additional free volume to the probe. The controlled location of chromophores at the site of maximum mobility may be fulfilled by means of a designed length of a tagging spacer.

Origin of Microheterogeneity in Solid Polymers. Interpretation of the inhomogeneous molecular motion should not contradict the following observations. (1) The fluorescence probe bonded to a polymer via a dodecyl spacer is more mobile than the monomeric probe simply mixed in the matrix. (2) The segment mobility is not governed by T_g . (3) The probe surrounded by long and bulky neighboring side chains loses mobility.

The sequence of R , poly(MMA-co-12) > poly(BMA-co-12) > poly(CHMA-co-12), is very suggestive, since the sequence of T_g is poly(MMA-co-12) > poly(CHMA-co-12) > poly(BMA-co-12) as shown in Table I. Thus, the possibility of a long alkyl chain playing the role of plasticizer is rejected. If this were the case, the R value of poly(BMA-co-12) should have been larger than that of poly(MMA-co-12). On the contrary, the long alkyl chains restrict the molecular motion of the TICT probe. The fact that poly(MMA-co-12) seems to indicate the existence of considerable free volume in between the polymer main chains as depicted in Figure 7. With an appropriate spacer length, the TICT probe in poly(MMA-co-12) will be situated in the most favorable location (Figure 7a). In the polymers with longer or bulkier alkyl side chains, the available space is filled with the side chain so that congestion around the TICT probe increases. Although the alkyl side chain is softer than the main chain, the space-filling effect predominates the plasticizing effect. The time range of measurements may be of importance. The for-

mation of the TICT state occurs within the time scale of picoseconds to nanoseconds. If we use other probes responding more slowly, the situation might be different.

There is a surprisingly good correlation between the fluorescence behaviors in dilute solutions^{2,3} and in the solid state. The absolute values of TICT emission are certainly different whereas the relative sequences of R values and REE in the solid state as a function of polymer structure are almost the same as for those in solution, particularly when the solvent is poor. Either in the presence or in the absence of solvent molecules, the microheterogeneity in polymers is likely to be of an intrinsic nature, relevant to the polymer main chain and the side chain.

As we have shown, there are considerable effects of polymer structure on the ground-state conformation. It is therefore questionable to what extent the change in the R value corresponds to the rate of forming the a^* state. In the present stage we cannot decide whether the polymer structural effect is static (i.e., effect on the ground-state conformation) or dynamic (i.e., effect on the rates of the excited-state processes). Time-dependent fluorescence spectroscopy to determine the rate of TICT state formation is now under way.

Acknowledgment. We thank Dr. R. Hayashi for the sample of poly(MMA-co-2) and Dr. N. Kitamura for his helpful discussion.

Registry No. (MMA)(2) (copolymer), 105058-53-5; (MMA)(4) (copolymer), 112925-61-8; (MMA)(8) (copolymer), 112925-62-9; (MMA)(12) (copolymer), 112925-63-0; (BMA)(12) (copolymer), 116911-34-3; (CHMA)(12) (copolymer), 116911-35-4; (DDMA)(12) (copolymer), 116911-36-5.

References and Notes

- (1) Visiting fellow from the Institute of Photographic Chemistry, Academia Sinica, Beijing, China.
- (2) Tazuke, S.; Guo, R. K.; Hayashi, R., *Macromolecules* **1988**, *21*, 1046.
- (3) Tazuke, S.; Guo, R. K.; Hayashi, R., *Macromolecules* **1989**, *22*, 729.
- (4) Winnik, M. A., Ed. *Photophysical and Photochemical Tools in Polymer Science*; Reidel: Dordrecht, Netherlands, 1987.
- (5) Hoyle, C. E.; Torkelson, J., Eds. *Photophysics of Polymer*; ACS Symposium Series 358, American Chemical Society: Washington, DC, 1987.
- (6) Birks, J. B. *Photophysics of Aromatic Molecules*; Wiley: London, 1970; Chapter 7 and 9.
- (7) (a) Tazuke, S.; Yuan, H. L. *Polym. J.* **1982**, *14*, 695. (b) Yuan, H. L.; Guo, R. K.; Zhen, J.; Tazuke, S. XII International Conference on Photochemistry; Tokyo, 1985; Abstract 317.
- (8) Grabowski, Z. R.; Rotkiewicz, K.; Rubaszewska, A.; Kirkor-Kamińska, E. *Acta Phys. Pol.* **1978**, *A54*, 767.
- (9) Rettig, W. *J. Lumin.* **1980**, *26*, 21.
- (10) Hayashi, R.; Tazuke, S.; Frank, C. W. *Macromolecules* **1987**, *20*, 983.
- (11) Hayashi, R.; Tazuke, S.; Frank, C. W. *Chem. Phys. Lett.* **1987**, *135*, 123.
- (12) Hayashi, R.; Tazuke, S.; Frank, C. W. *Photophysics of Polymers*; ACS Symposium Series 358, American Chemical Society: Washington, DC, 1987; p 135.
- (13) Al-Hassan, K. A.; El-Bayoumi, M. A. *Chem. Phys. Lett.* **1980**, *76*, 121.
- (14) Al-Hassan, K. A.; Rettig, W. *Chem. Phys. Lett.* **1986**, *126*, 273.
- (15) Horie, K.; Mita, I. *Chem. Phys. Lett.* **1982**, *93*, 61.
- (16) Horie, K.; Morishita, K.; Mita, I. *Macromolecules* **1984**, *17*, 1746.
- (17) Yu, W. C.; Sung, C. S. K. *Macromolecules* **1988**, *21*, 365.
- (18) Yu, W. C.; Sung, C. S. P.; Robertson, R. E. *Macromolecules* **1988**, *21*, 355.
- (19) Morawetz, H. *Science (Washington, D.C.)* **1988**, *240*, 172.
- (20) Torkelson, J. M.; Gilbert, S. R. *Macromolecules* **1987**, *20*, 1860.
- (21) Heskins, M.; Guillet, J. E. *Macromolecules* **1970**, *3*, 224.
- (22) Guillet, J. E. *Polymer Photophysics and Photochemistry*; Cambridge Univ. Press: Cambridge, 1985; (a) Chapter 2, (b) p 101.
- (23) Van-Ramesdonk, H. J.; Vos, M.; Verhoeven, J. M. *Polymer* **1987**, *20*, 983.

- (24) Farid, S.; Martic, P. A.; Thompson, D. R.; Specht, D. P.; Hartman, S. E.; Williams, J. L. R. *Pure Appl. Chem.* **1979**, *51*, 241.
- (25) Rettig, W.; Wermuth, G.; Lippert, E. *Ber. Bunsenges. Phys. Chem.* **1979**, *83*, 692.
- (26) Cazeau-Dubroca, C.; Peirigua, A.; Ait Lyazide, S.; Nouchi, G. *Chem. Phys. Lett.* **1983**, *98*, 511.
- (27) Cazeau-Dubroca, C.; Pririgua, A.; Ait Lyazidi, S.; Nouchi, G.; Cazeau, Ph.; Lapouyade, R. *Chem. Phys. Lett.* **1986**, *124*, 110.
- (28) Rotkiewicz, K.; Rubaszewska, W. *Chem. Phys. Lett.* **1980**, *70*, 444.
- (29) For recent discussion, see: Lippert, E.; Rettig, W.; Bonačić-Koutecký, V.; Heisel, F.; Miehe, J. A. *Adv. Chem. Phys.* **1987**, *68*, 1.

Global Equilibrium Configurations of Supercoiled DNA[†]

Ming-Hong Hao and Wilma K. Olson*

Department of Chemistry, Rutgers, the State University of New Jersey, New Brunswick, New Jersey 08903. Received December 2, 1988

ABSTRACT: The equilibrium configurations of circular DNA with imposed linking number differences are studied by computer simulation. The configurational energy of the double helix is described by an isotropic elastic deformation model together with a pairwise potential for calculating the self-interaction between distant points along the chain. The axis of the closed double-helical trajectory of the polymer is represented by piecewise cyclic B-spline curves that are approximated by a finite number of controlling points. The global minimum of the total potential energy is obtained with an algorithm that combines Metropolis-Monte Carlo sampling with a simulated annealing procedure. Simulation conditions are examined as are the effects of adjustable energy parameters. The dependence of the algorithm on temperature is related to the actual chain length of the DNA through the well-known relationship between persistence length and temperature. The predicted three-dimensional arrangements are consistent with the configurations of supercoiled DNA observed in electron micrographs. The most stable structures of the closed chain are found to be interwound configurations that are also critically dependent on the specified linking number difference. The toroidal configuration is found to be unstable and, upon energy minimization, is transformed to an interwound form. The optimized trajectories of knotted structures, however, are independent of the linking difference over the limited range of values examined.

Introduction

It is commonly observed in physical studies of naturally occurring closed circular DNA that a sample of homogeneous molecular weight resolves into three well-distinguished components: an intact ring, a nicked ring with one broken strand, and a linear duplex created by two single-strand breaks.¹⁻⁴ The linear DNA is well-known to behave as a Porod-Kratky wormlike chain.^{5,6} The same model can also be extended, with proper accounting of the ring-closure constraint, to the treatment of nicked DNA.^{6,7} An intrinsic supercoiling, however, overrides the configurational fluctuations of the double helix in intact naturally occurring circular DNA, with ordinary techniques of polymer configurational statistics becoming less effective, if not invalid. This supercoiling is attributed to a linking number difference with respect to the natural linking number of the relaxed double helix. The linking number is a topological parameter equal to the number of times one strand of the DNA links through the closed circle formed by the other strand.^{3,8-10} In relaxed circular DNA (e.g., the planar closed circle) the linking number is simply the winding number of the chain as measured by the number of residues divided by the intrinsic helical repeat. In supercoiled DNA, however, the linking number is a sum of the twisting of the chain about the helical axis plus the writhing of the folded helical trajectory.^{8,9} The linking number difference in a supercoiled duplex can only be relieved by chemical breakage of one of its two circular strands or by perturbation of the intrinsic helical repeat of the DNA through change of environment¹¹⁻¹⁴ or interaction with other molecules.^{4,15}

A useful approach in understanding DNA supercoiling is to characterize the configuration of the chain near its energy minimum. A convenient macroscopic model is provided by a long elastic rod, which when overtwisted and closed into a circle, folds into a unique three-dimensional shape. Various treatments¹⁶⁻¹⁹ have accordingly been offered to treat the supercoiling of DNA in a manner analogous to the treatment of the mechanical equilibrium of a twisted and closed elastic rod.^{20,21} Solutions to the three-dimensional arrangement of a linear rod have been explicitly obtained,^{17,22} and the solution to the circular rod problem has been discussed.^{22,23} The elastic equilibrium configurations of the closed rod are reported to be toroidal-like forms,²³ *n*-fold knots,²² and *n*-leafed roses.²² These elastic treatments, however, are still incomplete in the context of the DNA supercoiling problem in that no forces or torques other than those acting on the ends of the rod have been considered. Because closed circular DNA is usually interwound when examined under the electron microscope,²⁴ there is the possibility that the solution configuration of a supercoiled molecule may also adopt an interwound form.

A different approach to the supercoiling question is to consider the configuration of minimum deformation energy of a closed circular DNA with given linking number difference. Fuller has developed such a theory, predicting the interwound configuration to be a possible solution.⁹ Two different attempts, based on this formalism, have been recently offered to obtain solutions to the problem.^{25,26} The minimization of the deformation energy, however, leads to highly nonlinear equations that have been treated only by simplified variational methods (in which the helical parameters of the interwound helices are purposely specified as variational parameters). Even though such treatments are useful, they are clearly not the complete

[†] From the thesis submitted by Ming-Hong Hao in partial fulfillment of the requirements for the degree of Doctor of Philosophy, Rutgers, the State University of New Jersey, 1988.